Electronic Supplementary Material (ESI) for Inorganic Chemistry Frontiers.


**Exploring the effect of the reaction conditions on the mechanism of the photocatalytic reduction of $CO_2$ in vapor phase over $Pt/TiO_2$: An operando FTIR study**

Joudy Dankar, *[a,b] Virgile Rouchon,[a] Céline Pagis,[a] Mickael Rivallan,[a] Mohamad El-Roz*[b]

a) IFP Energies nouvelles, Rond-point de l'échangeur de Solaize, BP 3, 69360 Solaize, France. E-mail: joudy.dankar@ifpen.fr

b) Laboratoire Catalyse et Spectrochimie, Normandie Université, Caen, France. E-mail: mohamad.elroz@ensicaen.fr

# Supplementary Information

**Exploring the effect of the reaction conditions on the mechanism of the photocatalytic reduction of $CO_2$ in vapor phase over $Pt/TiO_2$: An operando FTIR study**

Joudy Dankar, *[a,b] Virgile Rouchon,[a] Céline Pagis,[a] Mickael Rivallan,[a] Mohamad El-Roz*[b]

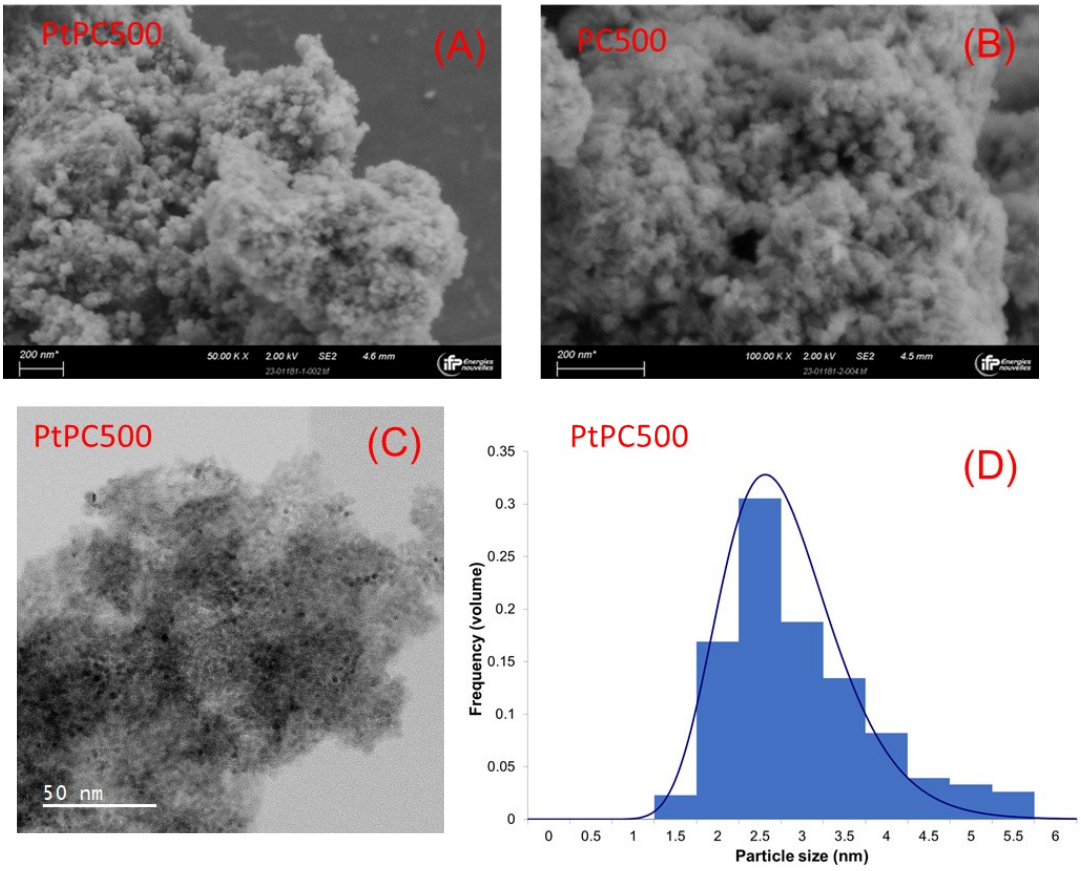


Figure S1. (A) Selected SEM images of 1 wt% $Pt/TiO_2$ prepared by photodeposition with 10 min deposition time and (B) bare $TiO_2$ (C) selected TEM image of 1 wt% $Pt/TiO_2$ and (D) corresponding platinum particle size distribution. Distribution charts was established on 414 measurements.

SEM images show that $TiO_2$ and $Pt/TiO_2$ display the same morphology. $TiO_2$ particles exist in the form of fairly dense grains measuring from 500 nm to several microns approximately. The latter consists of elementary particles measuring approximately 10 to 40 nm.

TEM BF was conducted with a spot size of 1 nm, probe current of 2.5 nA and a convergence angle of 21.3 mrad (100 µm condenser aperture). Images were recorded on a Gatan 4K OneView camera with typical integration times of 1s. HAADF/BF STEM was conducted with a probe size of 0.16 nm and current of 0.1 nA. Convergence was set to 20 mrad with a condenser aperture of 40µm. HAADF collection angle was of 24.4-89.4 mrad and BF of 9.8 mrad. Images were recorded with a 2K definition with a typical 10 µs integration per pixel. Particle size distribution (PSD) were calculated based on HAADF images at 2 Mx magnification by manually determining the size inventories of +200 individual particles with the help of an in-house software. PSD histograms were constructed using a 0.5 nm bin and calculated as the frequency of the numbers of objects. A log normal fit was applied to the data

to check for the quality of the distribution. The PSD is then given as the statistical average of the population with the standard deviation indicative of population spread.

The calculated histograms for particle size distribution shows a narrow particle size distribution of Pt with an average Pt nanoparticle size of 2.41 nm and standard deviation of 0.61.

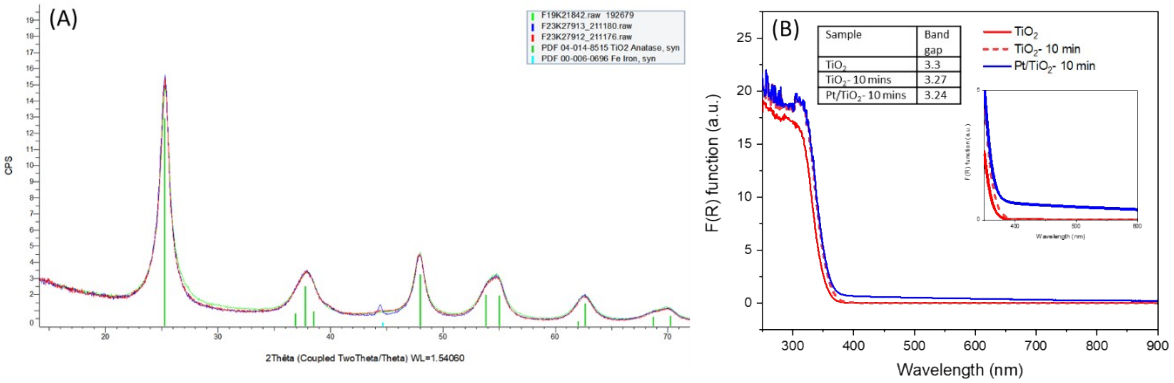


Figure S2. (A) XRD patterns for $TiO_2$, Pt/$TiO_2$ and spent Pt/$TiO_2$ (B) Diffuse reflectance UV-Vis spectra and calculated indirect band gap values of $TiO_2$, Pt/$TiO_2$, and $TiO_2$-control.

**Figure S2A:** XRD patterns reveal pure crystalline anatase phase before and after deposition of Pt. The average crystallite size calculated according to Scherrer method was similar before and after the photodeposition of platinum (bare $TiO_2$= 0.74 ± 0.8 nm, Pt/$TiO_2$= 0.80 ± 0.8 nm).

The spent Pt/$TiO_2$ sample following 180 min of reaction shows similar diffractogram as the fresh catalyst, except for an iron artifact coming from the sample holder (half-cell preparation of spent Pt/$TiO_2$ due to lack of powder). The $TiO_2$ crystalline structure and crystallite are maintained after 180 min of reaction (spent Pt/$TiO_2$= 0.79 ± 0.8 nm).

**Figure S2B:** Diffuse reflectance UV-vis absorption spectra were measured using an Agilent CARY 60 UV–vis spectrometer using BaSO4 as reference. Indirect band-gap energies were from the corresponding Kubelka–Munk functions, F(R), by plotting (F(R)·h$\nu$)1/2 against h$\nu$.

Resulting UV–vis diffuse reflectance spectra show a characteristic absorption threshold at wavelengths ~ 380 nm, implying that absorption is only in UV region, which is in line with the calculated intrinsic bandgap absorption of $TiO_2$ (3.3 eV). Pt/$TiO_2$ photocatalysts showed a slightly higher absorption than $TiO_2$ throughout the visible range (400–800 nm). Values of

indirect band gap energy for studied samples are calculated in the inset table in Figure S2B and reveal similar band gap energy values for all samples.

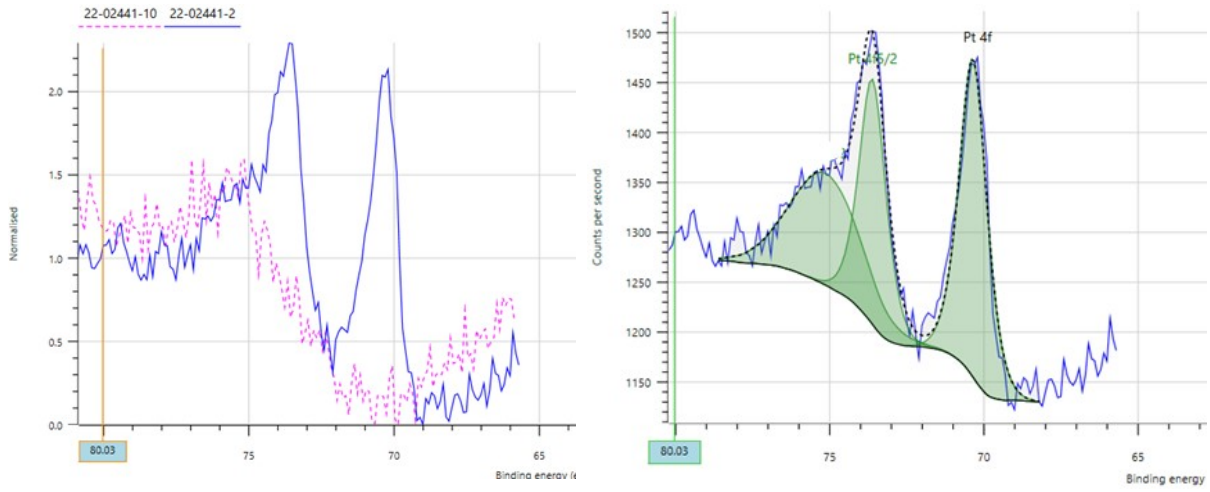


Figure S3. XPS Pt 4f region for 1 wt.% Pt-$TiO_2$ photocatalysts prepared with 10 min deposition time (blue solid line) and bare $TiO_2$ (pink dotted line).

The figures above report the Pt 4f spectra of the 1% Pt/$TiO_2$ s in blue and their corresponding support ($TiO_2$) in pink dotted lines. In addition to the Pt signal which presents 2 contributions Pt 4f7/2 and Pt 4f5/2 with a theoretical "spin orbit splitting" ratio of 3:4, a contribution towards 75 eV is observed. In addition to the Pt signal, a shoulder attributed to a secondary signal from Ti 3s interferes near the contribution Pt 4f5/2. For the exploitation of the data and the decomposition of the Pt signal, this surface has been integrated but is not included in the quantification.

The position of the main peak at ~70.3 eV is characteristic of platinum in the reduced state. A difference of 1.4 eV is proposed between the Pt° and $Pt^{2+}$ corresponding to platinum in the oxide state (PtO, Pt(OH), etc.). Such contribution is not found in the Pt/$TiO_2$-10 min sample, which shows that the majority of platinum occurs in a reduced metallic state ($Pt^0$). Therefore, platinum is in a fully reduced state following our adopted photodeposition procedure even after storage in atmospheric conditions.

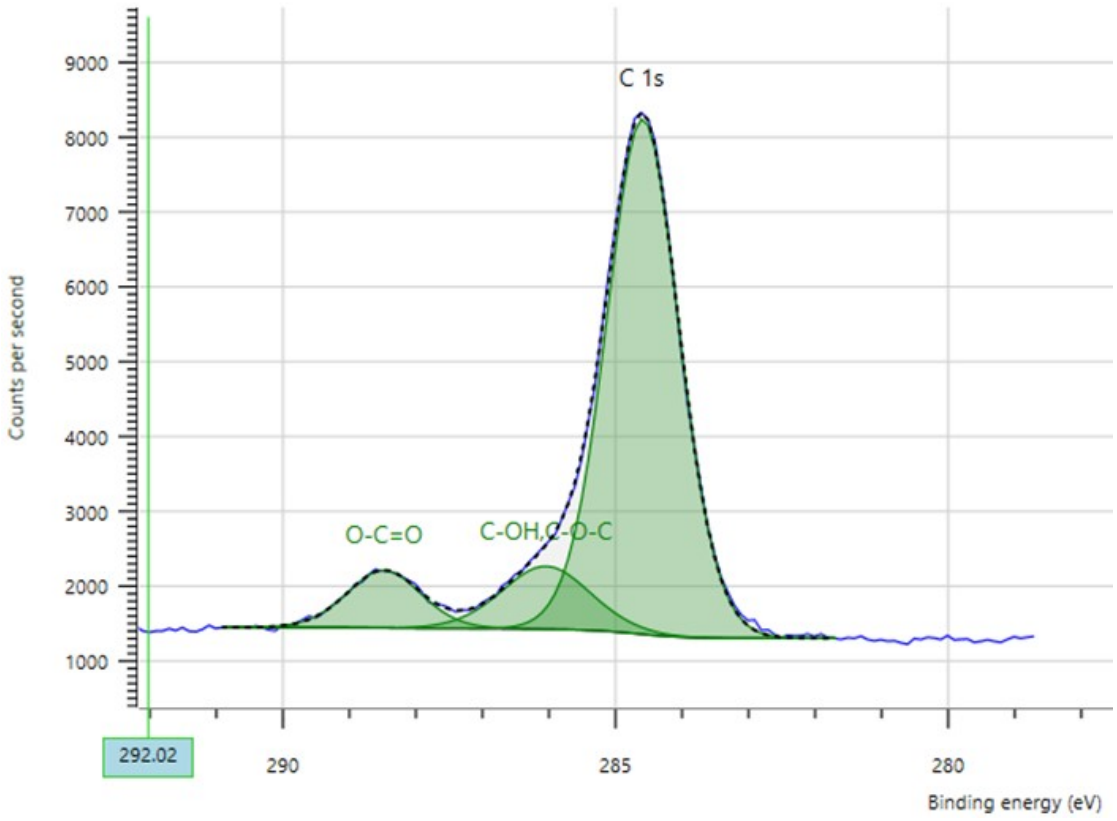


Figure S4. C 1s XPS spectrum for 1 wt.% $Pt/TiO_2$ photocatalyst prepared with 10 min deposition time.

Table S1: Relative proportion of the carbon contribution at 288.5 eV.

| Sample | % O-C=O/$C_{total}$ | Standard deviation |
|---|---|---|
| $Pt/TiO_2$ | 9.7 | 0.24 |
| $TiO_2$ | 8.1 | 0.31 |

Three main contributions are evidenced in the C 1s region: at 284.6 eV, 286.1 eV and 288.5 eV. While the contribution of contamination carbon cannot be eliminated, a relative comparison between O-C=O/$C_{total}$ ratio in bare $TiO_2$ and $Pt/TiO_2$ can confirm the relative enhancement in carboxylate species following photodeposition of Pt.

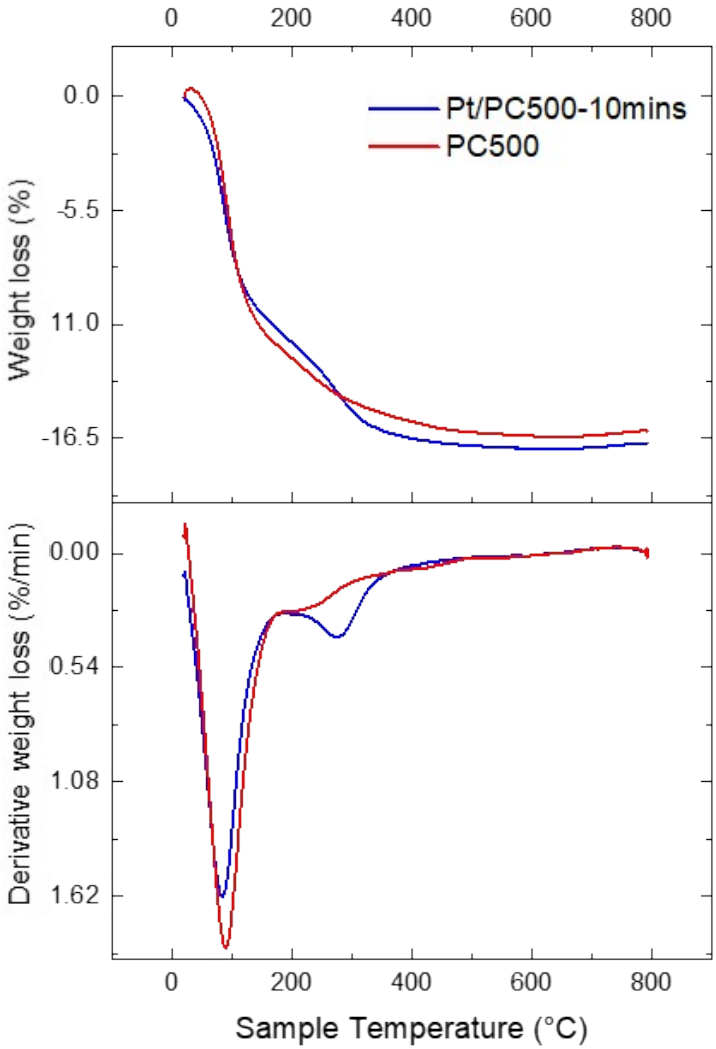


Figure S5. TGA and DTG analyses of a bare $TiO_2$ (red curve) and Pt/$TiO_2$ (blue curve) samples under 40 ml $min^{-1}$ air flow.

Humidity and carbon content of a bare $TiO_2$ and Pt/$TiO_2$ was studied by TGA-DTG using a heating program of 10 ºC/min up to 800 ºC under 40 ml $min^{-1}$ air flow.

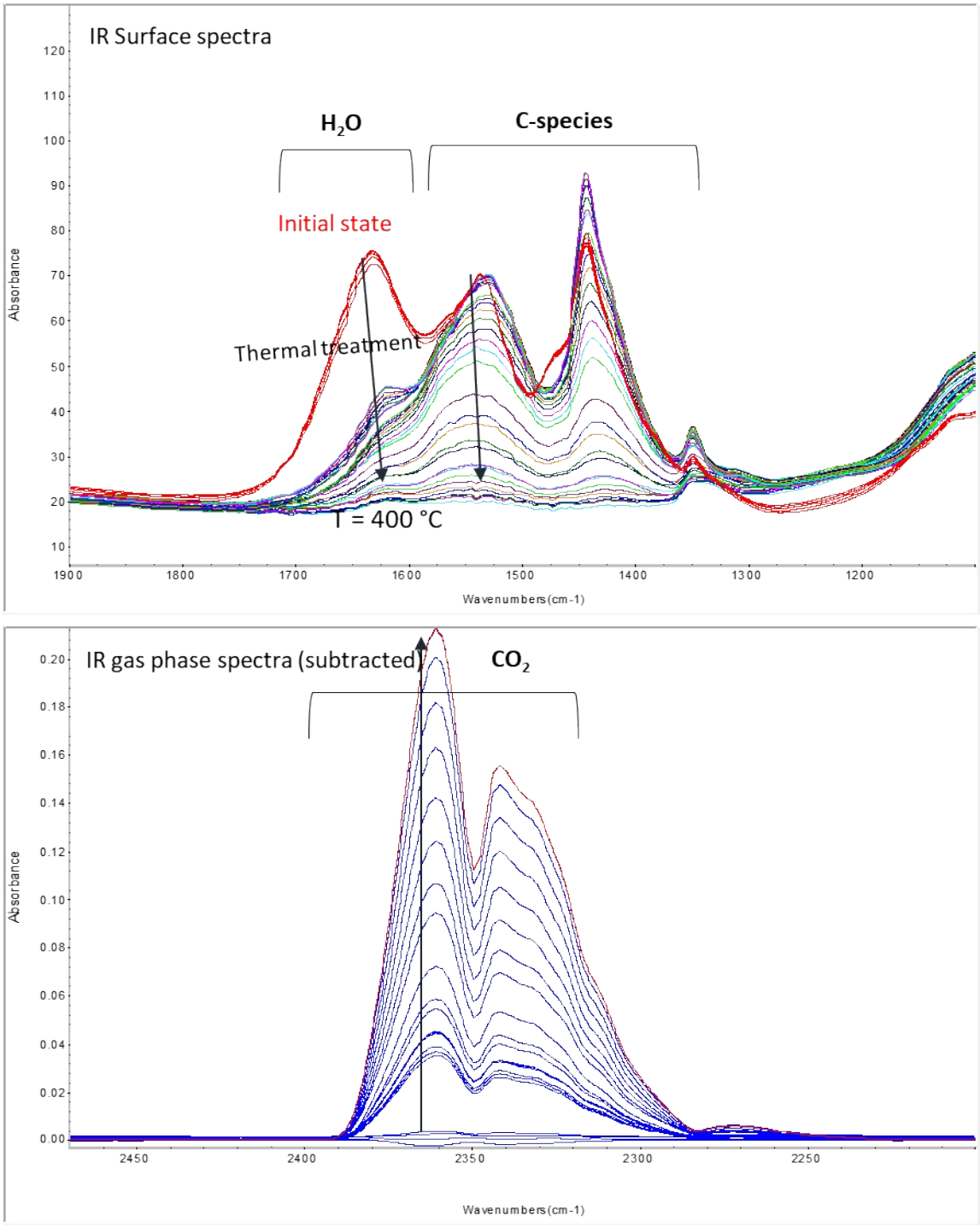


Figure S6. In situ thermal treatment coupled to FTIR spectroscopy of 1 wt% Pt/PC500- 10 mins under 15 ml $min^{-1}$ air flow at 5°C/min from RT to 400°C.

In situ IR spectra are recorded in surface and gas phase during thermal treatment under 15 ml $min^{-1}$ air flow at 5°C/min from RT to 400°C.

The doublet located between 2400 – 2200 $cm^{-1}$ reveals formation of $CO_2$ in gas phase.

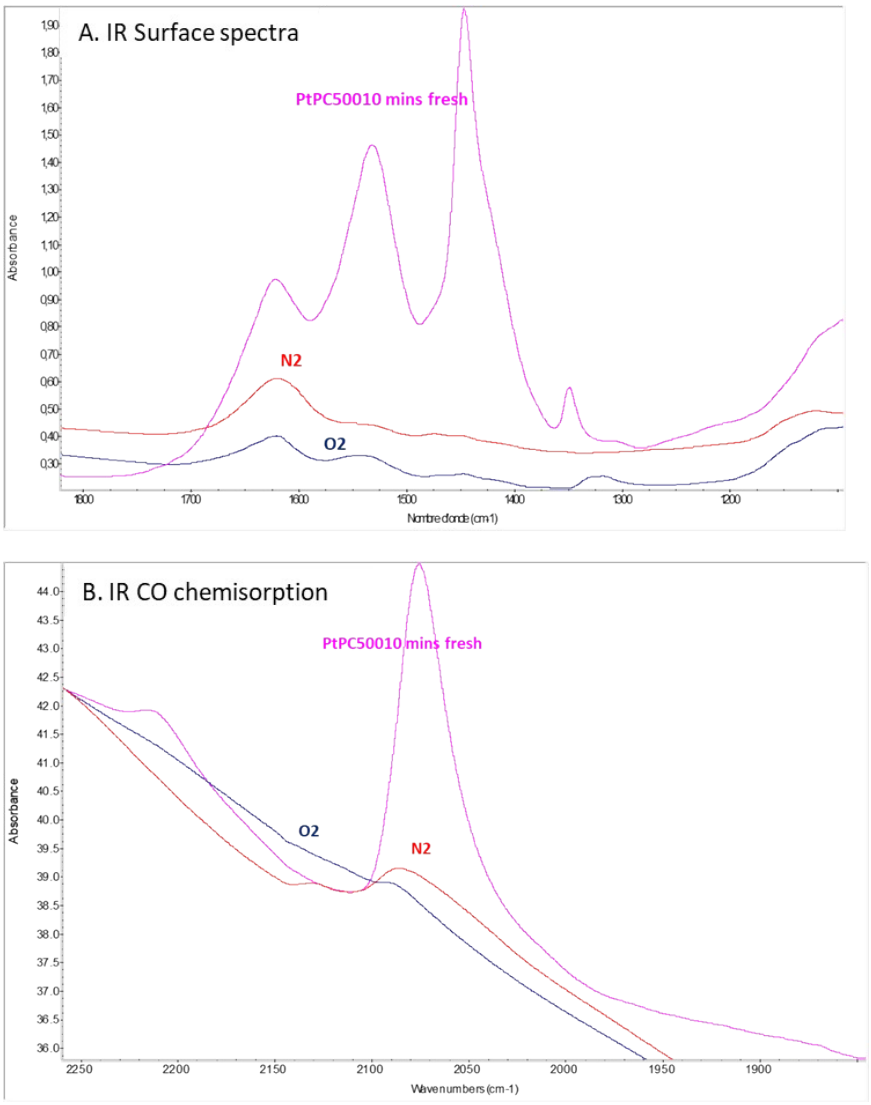


Figure S7. (A) FTIR surface spectra of fresh $Pt/TiO_2$ (pink) and that obtained after thermal treatment under $N_2$ at 300 °C (red) or under at 370 °C under $O_2$ (navy blue). (B) Corresponding FTIR spectra of CO adsorption of the samples at room temperature after reaching CO saturation.

**A. Surface state of thermally treated samples:** FTIR spectra following thermal post-treatment of the fresh $Pt/TiO_2$ sample under $N_2$ and $O_2$ reveal successful elimination of majority of C-species.

**B. Pt state followed by CO FTIR adsorption:** The FTIR spectra of CO adsorbed on metallic nanoparticles strongly depends on the nature of the metal and the treatment conditions of the catalyst. In the case of platinum, the IR spectrum obtained after CO adsorption located between 2100 $cm^{-1}$ and 2050 $cm^{-1}$ is assigned to linearly adsorbed CO on a metallic Pt atom ($CO – Pt^0$). The total amount of surface adsorbed CO after reaching CO saturation is displayed in Figure S7. The decrease in CO uptake following thermal treatment indicates the loss of accessible $Pt^0$ sites, which could be the results of oxidation and/or sintering of Pt NPs.

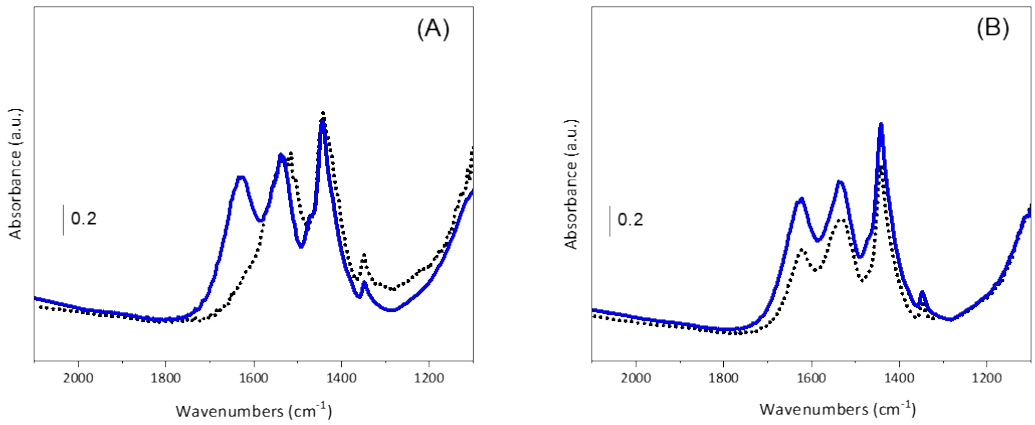


Figure S8: Steady state spectra before (blue) and after (dotted black) 1h-long irradiation of $Pt/TiO_2$ under (A) dry Ar and (B) wet Ar conditions.

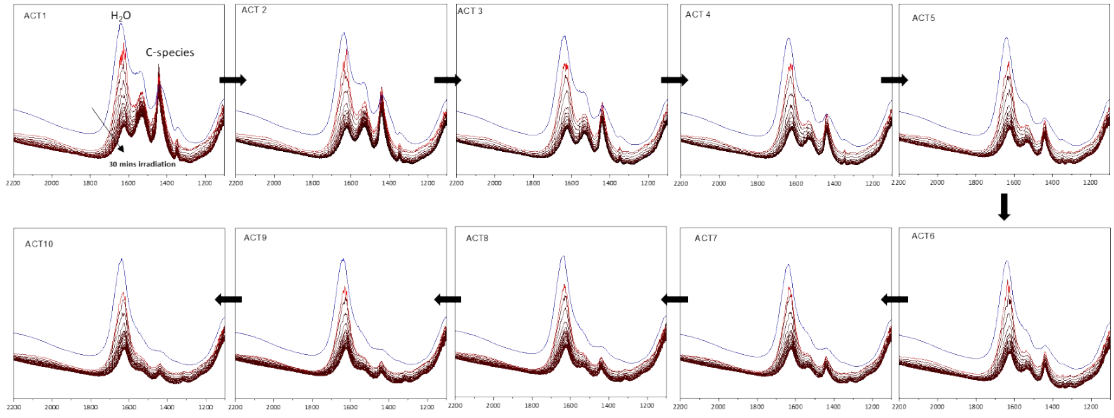


Figure S9. Operando FTIR spectra acquired during 10 successive light/dark cycles.

The catalyst surface is irradiated for 30 min until reaching steady state in the surface spectra. Afterwards, the catalyst is left in the dark until reaching steady state (i.e., around 60 min), after which it is irradiated again. The process is repeated ten times (i.e., 10 irradiation steps).

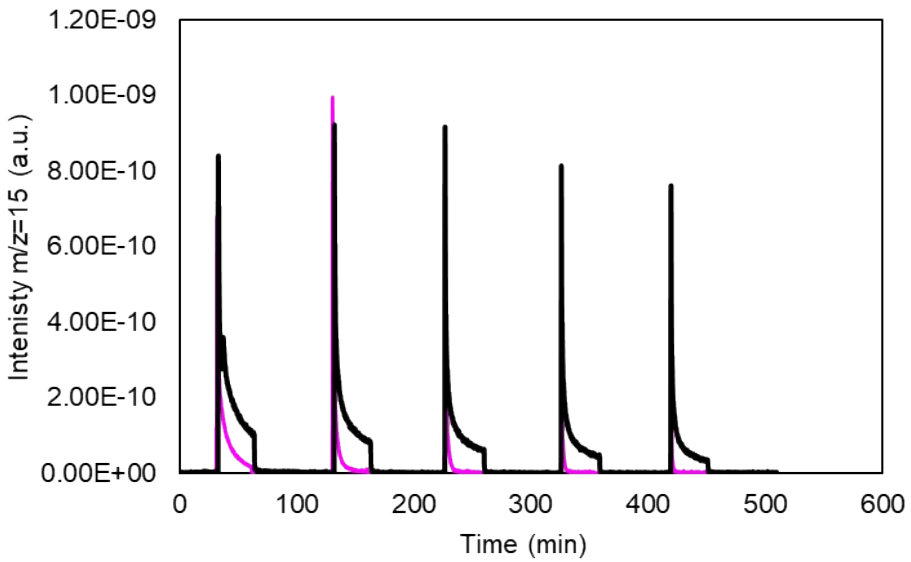


Figure S10. Instantaneous gas phase acquisition of methane recorded by mass spectrometer on m/z=15 for $Pt/TiO_2$ during 5 cycles of irradiation under humid Ar (pink curve) and under $CO_2$ with water (black curve).

The pink curve obtained under inert Ar indicates methane produced due to the conversion of impurities on the catalyst surface. The difference between black curve ($CO_2$ + $H_2O$) and the pink one (Ar + $H_2O$) is the real contribution of reactants on methane production.

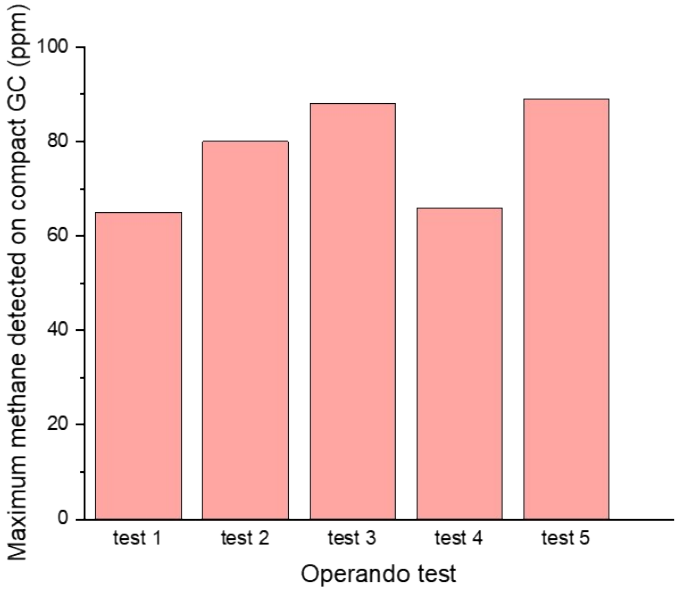


Figure S11. Maximum amount of methane detected on the compact GC in five operando $CO_2$ photoreduction tests for $Pt/TiO_2$.

Methane quantification from the operando photocatalytic experiments was performed using a compact gas chromatograph (GC) equipped with a flame ionization detector (FID) column. The compact GC conducted analyses at intervals of 6 minutes. Due to the rapid decline observed in methane levels by mass spectrometry (as depicted in Figure S10), the peak amount of methane recorded on the GC is reliant on the GC injection time. To assess methane production during $CO_2$ photoreduction, five tests were executed under identical conditions, and the highest methane quantity detected in each test is presented in Figure S11. The mean value corresponding to the methane peak from the five tests conducted in the operando setup is 78 ppm with a standard deviation of 11.6.

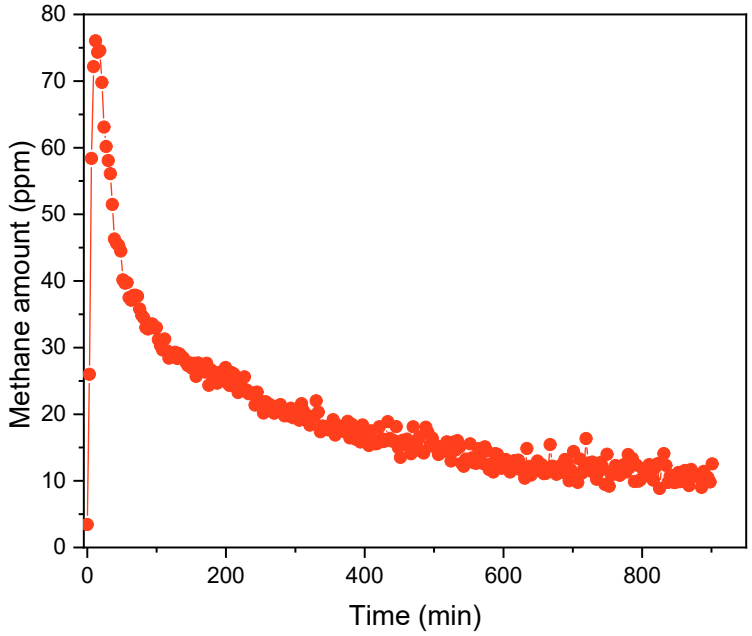


Figure S12. Methane evolution on GC during photocatalytic reduction of $CO_2$ with water under UV-Vis irradiation (λ = 280-620 nm) for $Pt/TiO_2$ using conditions comparable to operando set-up.

To ensure comparable and reproducible behaviour of the $Pt/TiO_2$ photocatalyst during $CO_2$ photoreduction, the conditions utilized in the photocatalytic unit were adapted to be similar to those utilized under *operando* test conditions. As such, 20 mg of catalyst in the form of self-supported pellets of 16 mm diameter were tested (instead of 300 g of powder). The lamp power was increased from 80 W/m² to 130 W/m², and the $CO_2$ flow rate was also adjusted from 0.3 cc/min to 5 cc/min. The amount of methane (ppm) detected MicroGC with a frequency of analysis every 3 min during 900 min irradiation is displayed in Figure S14. The maximum amount of methane detected under these conditions (76 ppm) is comparable to that obtained with the *operando* photoreactor (Figure S11).

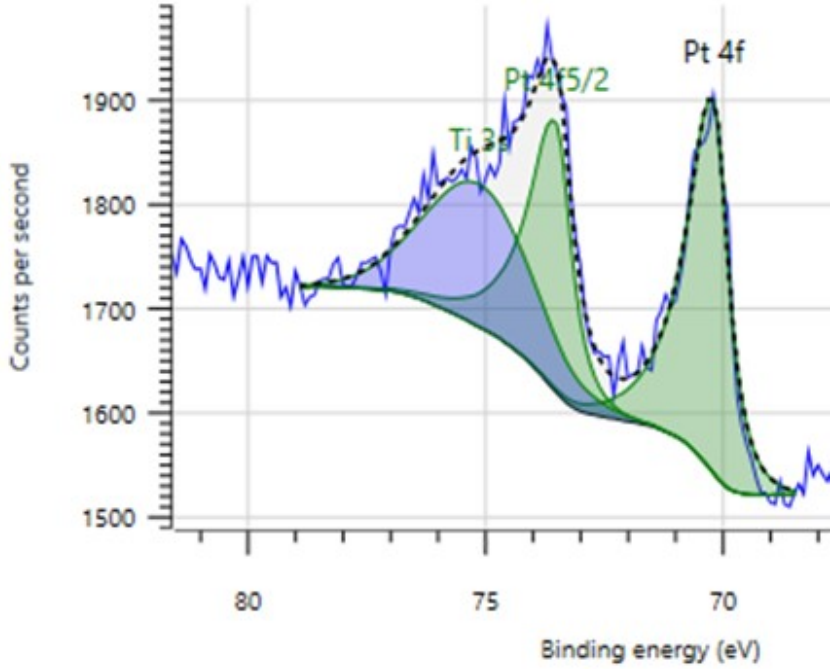


Figure S13. XPS Pt 4f region for used 1 wt.% Pt-$TiO_2$ photocatalyst after 180 min reaction.

The position of the main peak at ~70.3 eV is characteristic of platinum in the reduced state, which confirms that maintains its metallic state in the spent catalyst, even after 180 min of irradiation.

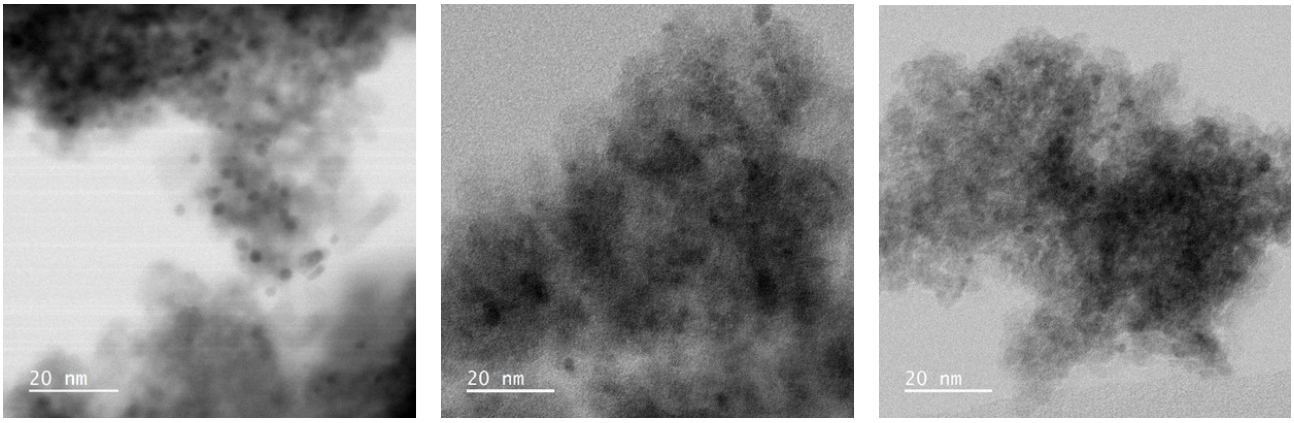


Figure S14. selected TEM images of spent 1 wt.% Pt-$TiO_2$ photocatalyst.

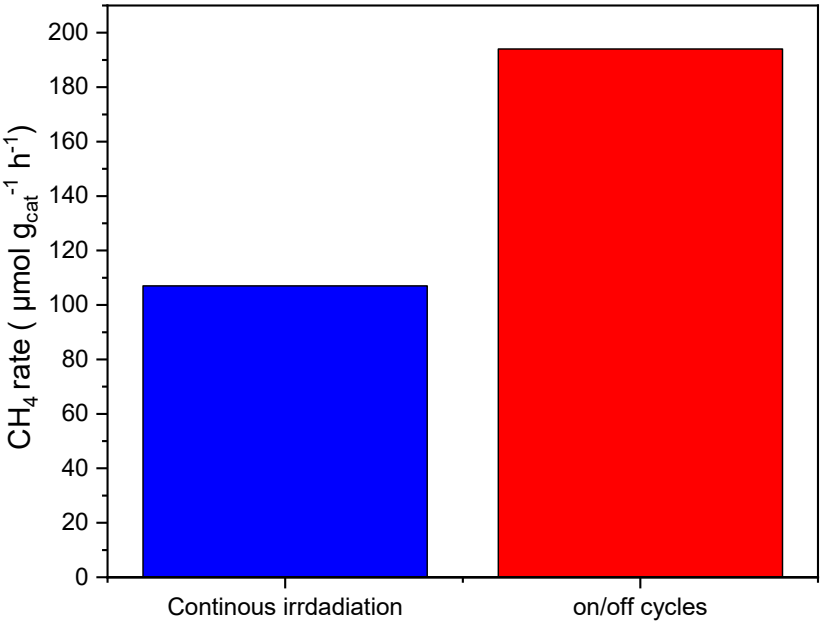


Figure S15. Amount of methane detected by GC FID channel during 180 min of continuous irradiation vs. on/off cycles of irradiation.